High-resolution grayscale image hidden in a laser beam

High-resolution grayscale image hidden in a laser beam

Fuyong Yue[1], Chunmei Zhang[1], Xiaofei Zang[1, 2], Dandan Wen[1], Brian D. Gerardot[1], Shuang Zhang[3†], Xianzhong Chen[1*]

1. *SUPA, Institute of Photonics and Quantum Sciences, School of Engineering and Physical Sciences, Heriot-Watt University, Edinburgh, EH14 4AS, UK*
2. *Shanghai Key Lab of Modern Optical System, University of Shanghai for Science and Technology, Shanghai, 200093, China*
3. *School of Physics and Astronomy, University of Birmingham, B15 2TT*

Abstract

Images as perceived by human eyes or recorded by cameras are usually optical patterns with spatially varying intensity or color profiles. Besides intensity and color, the information of an image can also be encoded in a spatially varying distribution of phase or polarization state. Interestingly, such images may not be viewed directly by human eyes or cameras as they may exhibit highly uniform intensity profiles. Here we propose and experimentally demonstrate an approach to hide a high-resolution grayscale image in a square laser beam with a size less than half a millimeter. An image with a pixel size of 300 nm by 300 nm is encoded into the spatially variant polarization states of the laser beam, which can be revealed after passing through a linear polarizer. This unique technology in hidden grayscale image and polarization manipulation renders new opportunities for a diverse range of applications including encryption, imaging, optical communications, quantum science, and fundamental physics.

Keywords: Grayscale image; metasurface; polarization manipulation

† Email: s.zhang@bham.ac.uk
* Email: x.chen@hw.ac.uk

Introduction

Images consisting of optical patterns with spatially varying intensity or color profiles can be perceived by human eyes or cameras. Besides intensity and color, the information of an image can also be encoded in a spatially varying distribution of polarization state. In this work, the first experimental demonstration of hiding a high-resolution grayscale image associated with a laser beam with a spatially inhomogeneous state of polarization is presented. Unlike optical holograms[1-3] and recently demonstrated color images in terahertz metasurfaces[4], where the information is encoded in the amplitude profile of the light beam, the image here is hidden in its polarization profile. For example, holograms are recorded interference patterns of construction (intensity peaks) and destruction (elimination) of the superimposed light wavefronts. However, the images in our work are encoded in the polarization profile of light beam with uniform intensity distribution. Figure 1 shows the schematic of our approach for hiding an image. A grayscale image is hidden in the structured beam with a spatially variant polarization profile, which is realized by a reflective metasurface illuminated by a laser beam at normal incidence. It should be noted that while only one reflected beam is shown in Figure 1 (for simplicity), two centro-symmetrically identical reflected beams are generated by the real device. An analyzer (linear polarizer) is used to reveal the hidden image in the generated structured beam. In memory of the milestone work of James Clerk Maxwell in electromagnetics, we take one of his grayscale portraits as the hidden image. Figure 1(a) and (b) show the simulation results with and without an analyzer, respectively. This approach allows us to conceal the high capacity information in the inhomogeneous polarization profile of the laser beam and transfer the hidden information along the propagation direction of the light. This simple approach may be applied to a variety of fields, including encryption, imaging, optical communications, quantum science, and fundamental physics.

Materials and Methods

According to Malus' Law, when a linearly polarized light beam passes through an analyzer (linear polarizer), the intensity of the light transmitted by the analyzer is directly proportional to the square of the cosine of angle θ between the transmission axes of the analyzer and the polarizer (see Figure 2(a)), i.e., $I = I_0\cos^2\theta$, where I_0 is the intensity of

incident light. A structured beam with inhomogeneous polarization distribution can generate a spatial intensity distribution when passing through a polarizer, providing a new degree of freedom to hide an image. Based on Malus' law, an arbitrary grayscale image can be hidden in the linear polarization profile of a light beam. Recently, metasurfaces[5-10] have enabled us to engineer the spatial distribution of amplitude, phase and polarization response at subwavelength resolution, allowing us to develop a plethora of ultrathin devices with unusual properties[6, 11-27].

Figure 2(b) shows the high-resolution grayscale image with 1300×1300 pixels that is to be hidden in the optical beam. The resultant beam has a dimension of 390 μm by 390 μm since each pixel has a size of 300 nm by 300 nm, exhibiting the subwavelength resolution. To explain our approach, we select an area from the eyebrow region with 10×10 pixels (Figure 2(c)). The enlarged intensity profile and the corresponding polarization distribution are given in the left and right of Figure 2(c) respectively. In our design, the transmission axes of the polarizer and the analyzer (polarizer) are respectively along horizontal and vertical directions.

The required light beam with an inhomogeneous linear polarization profile can be decomposed into the superposition of two circularly polarized beams with equal components and opposite handedness (Figure 2(d), (e)), which can be described as

$$\begin{aligned}\vec{\mathrm{E}}(x,y) &= E_0[\hat{x}\cos\varphi(x,y) + \hat{y}\sin\varphi(x,y)] \\ &= \tfrac{E_0}{\sqrt{2}}[\exp\big(i\varphi(x,y)\big)\,\hat{e}_R + \exp\big(-i\varphi(x,y)\big)\,\hat{e}_L]\end{aligned}$$

where $\varphi(x,y)$ represents the relative phase difference between the two orthogonal circular polarization states, and $\hat{e}_L = (\hat{x} + i\hat{y})/\sqrt{2}$ and $\hat{e}_R = (\hat{x} - i\hat{y})/\sqrt{2}$ are unit vectors of the left circular polarization (LCP) and the right circular polarization (RCP). A geometric metasurface is used to realize the handedness-dependent phase profile while maintaining constant amplitude[7, 16, 18, 28]. Here, a single reflective metasurface is designed to generate the desired structured beams by manipulating the superposition of two beams with opposite circular polarization states emerging from the identical metasurface (Figure 2(e)). The key point here is to generate a phase profile that, upon the illumination of RCP light, can

simultaneously generate a pair of centro-symmetrically distributed off-axis beams with same phase profile $\varphi(x, y)$. Since the sign of the geometric phase generated at the interface of metasurface depends on the handedness of the incident light, when the incident beam is changed from RCP to LCP, a pair of off-axis beams with the phase profile $-\varphi(x, y)$ are generated. Obviously, under the illumination of linearly polarized light beam which is the superposition of LCP and RCP components, the reflected beams with opposite handedness will meet and generate the desired polarization profile for the hidden images on both sides. Detailed explanation is given in Supplementary section 1. The combination of two sets of phase profiles for the two opposite incident handednesses will generate the desired polarization profile for the hidden image. In order to eliminate the effect of the non-converted beam, the off-axis configuration is used for metasurface design. Detailed explanation on the off-axis design is given in Methods and Supplementary section 1.

Results and Discussion

The design parameters of the metasurface and the fabrication process are presented in the Supplementary section 2. Figure 3(a) shows the scanning electron microscope (SEM) image of the part of the metasurface. In order to visualize the hidden image in the polarization topology of the laser beam, an analyzer (linear polarizer) is used to reveal the grayscale of the image. In doing so, we do not directly observe the spatially-variant polarization profile of the laser beam but rather indirectly confirm its existence through the intensity profile (grayscale image) behind the analyzer. For this metasurface, the additional phase difference between neighboring pixels to along x direction is $\pi/5$, where the corresponding reflection angle is 12.2^o (see Supplementary section 1). The experimental setup is given in Figure 3(b). An objective with a magnification of 10× is used to expand the image for visualization with a charge-coupled device (CCD) camera. Figure 3(c) and 3(d) show the simulation and experiment results. As shown by the numerical calculation, no image is observed in the intensity profile of the beam (Figure3(c) left). The experimental result, given in the right of Figure3(c), confirms that the image-hidden functionality is unambiguously realized. A high-quality image is revealed (Figure 3(d) right) with the analyzer whose transmission axis is along the vertical direction, which agrees with the simulation result very well (Figure 3(d) left). Here the transmission axes of the polarizer

and the analyzer are along horizontal and vertical directions, respectively. It should be noted that the incident light beam for the simulation is a plane wave with uniform intensity, whereas the incident beam for experiment is a collimated laser beam with Gaussian profile. It causes a slight discrepancy between experiment and simulation. Another reason for the discrepancy is the imperfection of linear polarizer and fabrication error. Due to the off-axis design, another identical image is also observed in the reflected beam on the other side with respect to the surface normal. The clear image of the moustache, eyeball and eyebrow indicates the ultrahigh resolution of the proposed approach. To further analyze the performance of our approach, the dependence of simulated and measured results on the direction of transmission axis of the analyzer is given in Figure 3(e). From the results at 0^o, 90^o, 45^o, 135^o, a good agreement between experimental and simulation results is found. Interestingly, the two images for the analyzer with orthogonal directions of transmission axis (e.g., 0^o and 90^o, 45^o and 135^o) are complementary grayscale images, i.e., the brightest area becomes the darkest area and vice versa. The evolution process of the revealed images can be seen clearly by gradually rotating the analyzer (see the video in the Supplementary movie S1).

To better understand the image hidden approach, we also study the dependence of image on the incident polarization state and the transmission axis of the analyzer. Although our design is based on the linear polarization, the device also works for the elliptical polarization since an elliptically polarized light can be decomposed into LCP light and RCP light with different components. However, the image quality will be deteriorated. The numerically calculated and experimentally observed images hidden in the laser beam are given under different circumstances (see Supplementary section 3). The measured hidden images with various combinations of the linear polarizer and the analyzer are also given in the Supplementary section 3.

Benefiting from the broadband nature of the geometric metasurface, the developed device can operate in a broad wavelength range. Images at different wavelengths are captured and given in Figure 4(a)-(f). The experimentally revealed clear images at the wavelengths of 500 nm, 550 nm, 575 nm, 600 nm, 640 nm and 700 nm unambiguously show the operation

of the developed device in the broad spectral range. The uniqueness of our approach lies in the encoding process of a high-resolution grayscale image onto the polarization profile of the laser beam. The image can be hidden and carried by a laser beam during light propagation, and can be revealed by an analyzer. We explore the performance of the approach for long distance propagation in free space (Figure 4(g)). Figure 4(h) presents the measured images after 4 meters' propagation in free space. The image can still be clearly seen although there is a slight change in the image quality.

The obtained image shows how the electric field is oriented in the beam profile of the laser beam. These hidden images demonstrate the rich polarization structure that a light beam can possess at subwavelength scales. The conversion efficiency is calculated by the power of the two resultant off-axis beams divided by that of the incident light. The efficiency in the wavelength range of 640 – 960 nm is given in Figure S7 and the maximum conversion efficiency is 60% at the wavelength of 820 nm (see Supplementary section 4).

Conclusions

Our approach provides a novel route to hide a high-resolution grayscale image in the polarization topology of a laser beam that has not previously been reported in the literature. The uniqueness of our approach in image hidden and precise polarization manipulation and high performance in resolution, bandwidth, and compactness renders this technology very attractive for diverse applications such as encryption, imaging, anti-counterfeiting, optical communications, quantum science, and fundamental physics.

Acknowledgments

This work is supported by the Engineering and Physical Sciences Research Council of the United Kingdom (Grant Ref: EP/M003175/1) . X. Z. acknowledge the support from the Chinese Scholarship Council (CSC, No. 201608310007).

X. C., F. Y., and S. Z. initiated the idea. F. Y., C. Z., and D. W. conducted the numerical simulations. F. Y. fabricated the samples. F. Y., C. Z. and X. Z. performed the

measurements. All the authors discussed and analysed the results. X. C. and S. Z. supervised the project. All the authors prepared the manuscript.

References

1. Zheng GX, Muhlenbernd H, Kenney M, Li GX, Zentgraf T*, et al.* Metasurface holograms reaching 80% efficiency. *Nat. Nanotechnol.* 2015; **10**(4)**:** 308-312.

2. Wang L, Kruk S, Tang H, Li T, Kravchenko I*, et al.* Grayscale transparent metasurface holograms. *Optica* 2016; **3**(12)**:** 1504.

3. Huang Y-W, Chen WT, Tsai W-Y, Wu PC, Wang C-M*, et al.* Aluminum plasmonic multicolor meta-hologram. *Nano Lett.* 2015; **15**(5)**:** 3122-3127.

4. Chanana A, Paulsen A, Guruswamy S, Nahata A. Hiding multi-level multi-color images in terahertz metasurfaces. *Optica* 2016; **3**(12)**:** 1466.

5. Yu N, Genevet P, Kats MA, Aieta F, Tetienne J-P*, et al.* Light propagation with phase discontinuities: generalized laws of reflection and refraction. *Science* 2011; **334**(6054)**:** 333-337.

6. Kildishev AV, Boltasseva A, Shalaev VM. Planar photonics with metasurfaces. *Science* 2013; **339**(6125)**:** 1232009.

7. Huang L, Chen X, Muhlenbernd H, Li G, Bai B*, et al.* Dispersionless phase discontinuities for controlling light propagation. *Nano Lett.* 2012; **12**(11)**:** 5750-5755.

8. Estakhri NM, Alù A. Recent progress in gradient metasurfaces. *J. Opt. Soc. Am. B* 2016; **33**(2)**:** A21-A30.

9. Yu N, Capasso F. Flat optics with designer metasurfaces. *Nat. Mater.* 2014; **13**(2)**:** 139-150.

10. Genevet P, Capasso F, Aieta F, Khorasaninejad M, Devlin R. Recent advances in planar optics: from plasmonic to dielectric metasurfaces. *Optica* 2017; **4**(1)**:** 139-152.

11. Ma HF, Shen X, Cheng Q, Jiang WX, Cui TJ. Broadband and high‐efficiency conversion from guided waves to spoof surface plasmon polaritons. *Laser Photon. Rev.* 2014; **8**(1)**:** 146-151.

12. Yu N, Aieta F, Genevet P, Kats MA, Gaburro Z*, et al.* A broadband, background-free quarter-wave plate based on plasmonic metasurfaces. *Nano Lett.* 2012; **12**(12)**:** 6328-6333.

13. Jiang S-C, Xiong X, Hu Y-S, Hu Y-H, Ma G-B*, et al.* Controlling the Polarization State of Light with a Dispersion-Free Metastructure. *Phys. Rev. X* 2014; **4**(2).

14. Lin D, Fan P, Hasman E, Brongersma ML. Dielectric gradient metasurface optical elements. *Science* 2014; **345**(6194)**:** 298-302.

15. Arbabi A, Horie Y, Bagheri M, Faraon A. Dielectric metasurfaces for complete control of phase and polarization with subwavelength spatial resolution and high transmission. *Nat. Nanotechnol.* 2015; **10**(11)**:** 937-943.

16. Chen X, Huang L, Muhlenbernd H, Li G, Bai B*, et al.* Dual-polarity plasmonic metalens for visible light. *Nat. Commun.* 2012; **3:** 1198.

17. Chen WT, Yang K-Y, Wang C-M, Huang Y-W, Sun G*, et al.* High-efficiency broadband meta-hologram with polarization-controlled dual images. *Nano Lett.* 2013; **14**(1)**:** 225-230.

18. Khorasaninejad M, Chen WT, Devlin RC, Oh J, Zhu AY*, et al.* Metalenses at visible wavelengths: Diffraction-limited focusing and subwavelength resolution imaging. *Science* 2016; **352**(6290)**:** 1190-1194.

19. Guo R, Rusak E, Staude I, Dominguez J, Decker M*, et al.* Multipolar coupling in hybrid metal–dielectric metasurfaces. *ACS Photonics* 2016; **3**(3)**:** 349-353.

20. Yin X, Ye Z, Rho J, Wang Y, Zhang X. Photonic spin Hall effect at metasurfaces. *Science* 2013; **339**(6126)**:** 1405-1407.

21. Lin J, Mueller JB, Wang Q, Yuan G, Antoniou N*, et al.* Polarization-controlled tunable directional coupling of surface plasmon polaritons. *Science* 2013; **340**(6130)**:** 331-334.

22. Ye W, Zeuner F, Li X, Reineke B, He S*, et al.* Spin and wavelength multiplexed nonlinear metasurface holography. *Nat. Commun.* 2016; **7**.

23. Grady NK, Heyes JE, Chowdhury DR, Zeng Y, Reiten MT*, et al.* Terahertz metamaterials for linear polarization conversion and anomalous refraction. *Science* 2013; **340**(6138)**:** 1304-1307.

24. Ni X, Wong ZJ, Mrejen M, Wang Y, Zhang X. An ultrathin invisibility skin cloak for visible light. *Science* 2015; **349**(6254)**:** 1310-1314.

25. Genevet P, Yu N, Aieta F, Lin J, Kats MA*, et al.* Ultra-thin plasmonic optical vortex plate based on phase discontinuities. *Appl. Phys. Lett.* 2012; **100**(1)**:** 013101.

26. Ni X, Ishii S, Kildishev AV, Shalaev VM. Ultra-thin, planar, Babinet-inverted plasmonic metalenses. *Light Sci. Appl*. 2013; **2**(4)**:** e72.

27. Yue F, Wen D, Zhang C, Gerardot BD, Wang W*, et al.* Multichannel Polarization‐Controllable Superpositions of Orbital Angular Momentum States. *Adv. Mater.* 2017.

28. Wen D, Yue F, Li G, Zheng G, Chan K*, et al.* Helicity multiplexed broadband metasurface holograms. *Nat. Commun.* 2015; **6:** 8241.

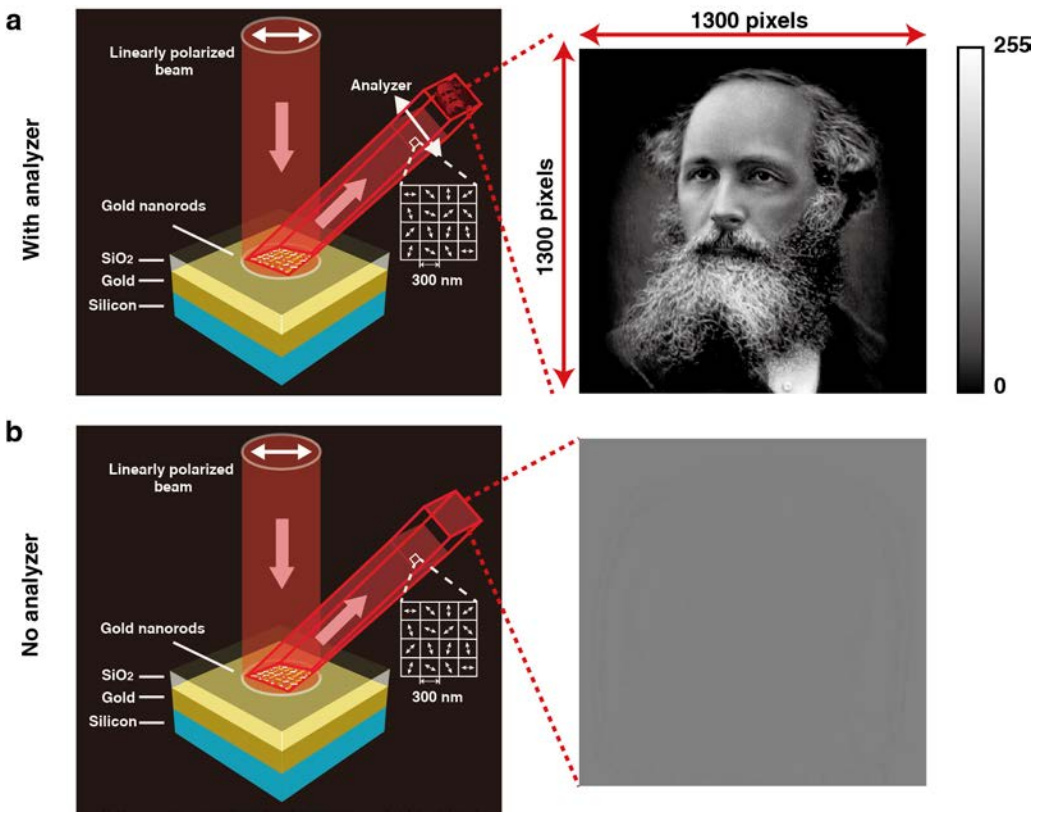

Figure 1. The schematic for hiding a high-resolution grayscale image. Under the illumination of linearly polarized light, two reflected beams with a spatially variant linear polarization profile are generated, which can be used to hide a high-resolution grayscale image (1300×1300 pixels and 256 grayscale levels). It is worth mentioning that only one reflected beam is shown here for demonstration. The two beams are exactly the same apart from the propagation direction. The hidden image is revealed by an analyzer (linear polarizer) (**a**), while no image is obtained without it (**b**). The metasurface consists of gold nanorods with spatially varying orientations on the top, a SiO_2 spacer (85 nm) and a gold background layer (150 nm) resting on a silicon substrate. The grayscale image is encoded into the polarization profile of the resultant beam at subwavelength scale via the metasurface. The size of each pixel is 300 nm×300 nm and the overall size of image is 390 μm ×390 μm.

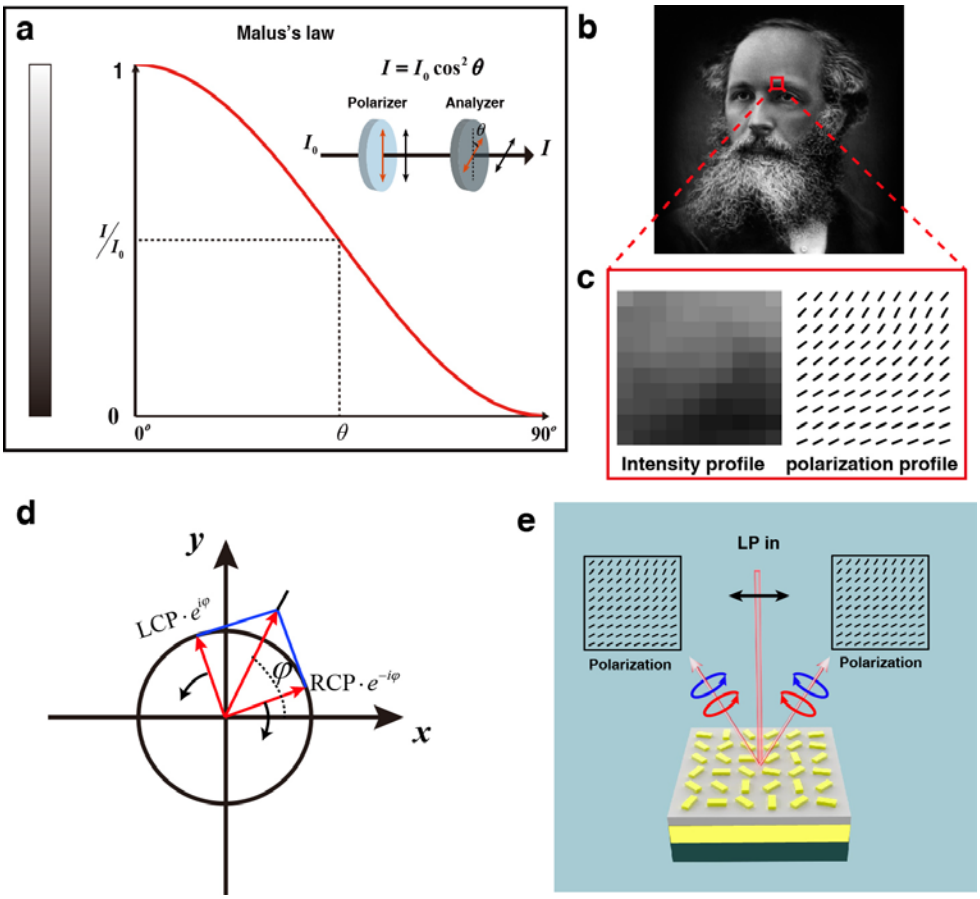

Figure 2. Malus' law and image hidden mechanism. (**a**) According to Malus' Law, when a linearly polarized light beam passes through an analyzer (linear polarizer), the intensity of light transmitted by the analyzer is $I = I_0\cos^2\theta$. Where I_0 is the intensity of incident light and θ is the angle between the transmission axes of the analyzer and the polarizer. A grayscale image is hidden in the linear polarization profile of a light beam. (**b**) The target image of James Clerk Maxwell's grayscale portrait. (**c**) The details of selected area from the eyebrow area with 10×10 pixels. The left side shows the grayscale profile and the right side shows the required polarization distribution for the analyzer with a transmission axis along the vertical direction. (**d**) A linear polarization is generated by a coherent superposition of two planar circularly polarized beams with opposite handedness, propagating along the same direction. (**e**) Since the sign of the geometric phase generated at the interface of metasurface only depends on the handedness of the incident light, under the illumination of a linearly polarized beam, the off-axis reflected beams with opposite handedness will meet and interfere with each other, generating the desired polarization profile for the hidden image on both sides.

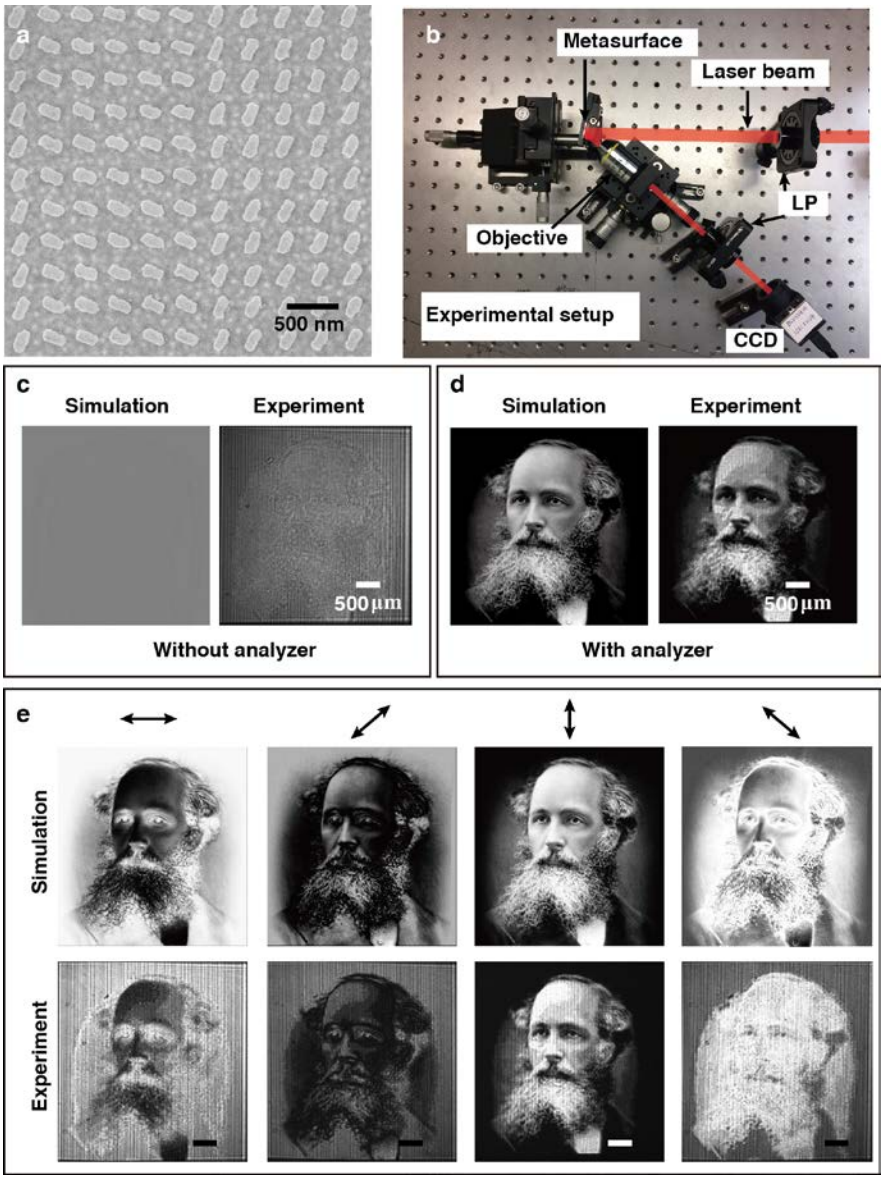

Figure 3. Fabricated metasurface, experiment setup and metasurface device characterization. (**a**) The SEM image of the fabricated metasurface. The scale bar is 500 nm. (**b**) The experimental setup. The collimated light beam with the required linear polarization is generated using a linear polarizer (LP), and then is incident on the metasurface which is mounted on a 3D translation stage. An objective with a magnification of 10X is used to collect and expand the resultant beam. The images are captured by the charge-coupled device (CCD). The analyzer, which is a linear polarizer, is placed in front of the CCD to reveal the hidden image. The simulated and experiment results without (**c**) and with the analyzer (**d**). Note that the direction the transmission axis is along vertical direction. (**e**) The simulated and experimental results for the analyzer with various directions of transmission axis. Results at 0^o, 45^o, 90^o, 135^o are given. The scale bar is 500 μm .

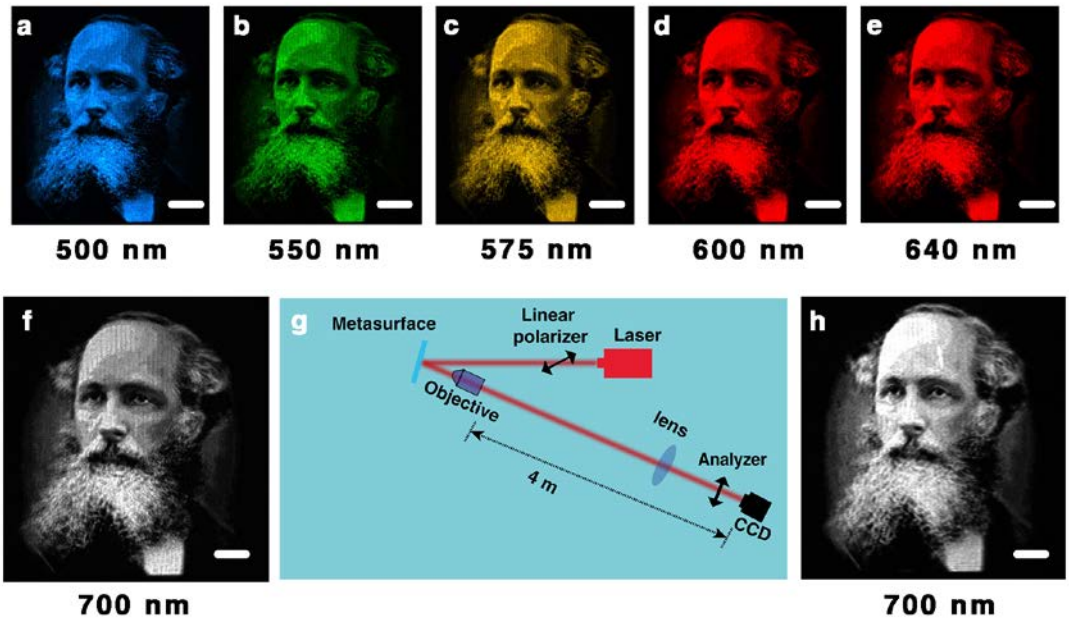

Figure 4. Broadband performance and robustness of the proposed approach. The experimental results at the wavelengths of (**a**) 500 nm, (**b**) 550 nm, (**c**) 575 nm, (**d**) 600 nm, (**e**) 640 nm, (**f**) 700 nm. (**g**) The experimental setup for the characterization of the hidden image for long distance propagation. (**h**) The obtained image after propagating 4 m in free space. Scale bar, 500 μm . The images of (a-e) are captured by the color CCD with pixel numbers 1024×768. The images of (f) and (h) are captured by the monochrome CCD with pixel numbers 1280×1024.